NUMERICAL SIMULATION OF THE DYNAMICS OF AN INTENSE RELATIVISTIC BEAM OF CHARGED PARTICLES

V. B. Bavin, V. M. Vetsko, V. A. Leitan,
A. S. Roshal', and A. V. Shal'nov

UDC 621.384.6

A method for the numerical simulation of stochastic processes in intense relativistic beams of particles moving in electric and magnetic fields is described. A two-dimensional approximation using "coarse particles" is considered. The action functions are first tabulated with respect to three variables. The method combines high speed and good accuracy. The results of a simulation are presented.

1. Numerical simulation on a computer using coarse particles is an effective method of investigating processes which occur in ensembles of particles [1-5]. In the case of a relativistic beam the calculations are complicated by the fact that the space-charge forces produced by the particles depend on their position and on their velocity. The Coulomb interaction forces between the particles can be calculated using the so-called action functions of the particles. The volume of calculations is proportional to the square of the number of coarse ("computer") particles. Hence, the permissible number of computer particles is of necessity limited and in the best computers does not exceed several hundred. The memory of a computer is fairly large and enables one to store a vast amount of data, which can be used to speed up the solution of the equations of motion and of the field using suitable algorithms.

We will consider the propagation of particles of charge e and rest mass m_0 in a cylindrical region consisting of a drift space and an interaction space in which interaction occurs with a traveling electromagnetic wave. (The boundary at the junction of the drift region and the interaction region is assumed to be arbitrary and is the cross section in which the high-frequency electromagnetic wave is introduced. The weak nonsynchronous interaction with this wave in the drift region is ignored.) It is assumed that in the drift space bunches of particles are formed (in accordance with the injection algorithm) with certain assigned coordinate and velocity distribution functions. By assigning different distribution functions we can study their effect on the processes. After drifting, the bunches arrive in the interaction region which is a cylindrical waveguide containing irises. In the interaction region the beam is close to synchronism and interacts strongly with the fundamental space harmonic of the traveling microwave field which has a wavelength in free space λ and a phase velocity $v_W = \beta_W c$ (c is the velocity of light).

We will assume that the problem is axially symmetric, that the beam does not perturb the external electromagnetic field, and that the longitudinal component of the external magnetic field depends only on the longitudinal coordinate. The radiation of the particles is ignored. The computer particles of charge Me and rest mass Mm_0 are represented in the form of infinitely thin rings, the radius of which can be varied during the course of the simulation. The charge of the rings Me and the number of the injected particles n(0) are chosen in such a way that the current of the beam in the model is the same as in the physical system. During the course of the simulation the particles may leave the region (for example, they may hit the walls of the tube, the target, etc.). The number of particles remaining in the region at the instant of time τ, will be denoted by $n(\tau) \leq n(0)$.

At each instant of time τ we calculate the space-charge field from the known coordinates and velocities of all the $n(\tau)$ particles. Then, from the equations of motion we find the coordinates and velocities of the particles at the instant of time $\tau + \Delta\tau$.

Moscow. Translated from Zhurnal Prikladnoi Mekhaniki i Tekhnicheskoi Fiziki, No. 6, pp. 61-66, November-December, 1973. Original article submitted March 29, 1973.

The equation of motion of a relativistic particle

$$\frac{d\mathbf{v}}{d\tau} = \frac{e}{m_0}\sqrt{1-\left(\frac{v}{c}\right)^2}\left\{\mathbf{E} + [\mathbf{v}\mathbf{B}] - \frac{1}{c^2}\mathbf{v}(\mathbf{v}\mathbf{E})\right\} \tag{1.1}$$

in a cylindrical system of coordinates $\{r, \theta, z\}$, after changing to the dimensionless variables

$$t = \frac{c\tau}{\lambda}, \quad \xi = \frac{z}{\lambda}, \quad \eta = \frac{r}{\lambda}, \quad \alpha = \frac{r}{c}\frac{d\theta}{d\tau} \tag{1.2}$$

takes the form

$$\begin{aligned}
\xi'' &= F_\xi(t) \equiv \frac{1}{\gamma}[E_\xi + \eta' B_\alpha - \alpha B_\eta - \xi'(E_\xi\xi' + \eta' E_\eta)] \\
\eta'' &= F_\eta(t) \equiv \frac{1}{\gamma}[E_\eta - \xi' B_\alpha + \alpha B_\xi - \eta'(E_\xi\xi' + \eta' E_\eta)] + \frac{\alpha^2}{\eta} \\
\alpha' &= F_\alpha(t) \equiv \frac{1}{\gamma}[-\eta' B_\xi + \xi' B_\eta - \alpha(E_\xi\xi' + \eta' E_\eta)] - \frac{\alpha\eta'}{\eta}
\end{aligned} \tag{1.3}$$

where the prime denotes differentiation with respect to t, and γ is the Lorentz factor:

$$\gamma = (1-\beta^2)^{-1/2}, \quad \beta^2 = (\xi')^2 + (\eta')^2 + \alpha^2 \tag{1.4}$$

The axial component $E_\theta = 0$. When changing from dimensionless field strength to dimensional field strength they must be multiplied by the corresponding normalizing factors:

$$E_{z,r} = \frac{m_0 c^2}{c\lambda} E_{\xi,\eta}, \quad B_{z,r,\theta} = \frac{m_0 c}{c\lambda} B_{\xi,\eta,\alpha}$$

We can add the following equation for the phase to Eqs. (1.3):

$$\varphi = \varphi_0 - 2\pi t + \Phi(\xi), \quad \Phi(\xi) = 2\pi\int_{\xi_0}^{\xi}\frac{d\xi}{\beta_w(\xi)} \tag{1.5}$$

where φ_0 is the phase of the wave of the external electromagnetic field at the input to the interaction space ξ_0 at the initial instant t = 0.

The fields **E**, **B** in the equation of motion (1.1) are made up of external fields $\mathbf{E}_w$ and $\mathbf{B}_w$, and the space-charge fields $\mathbf{E}_s$ and $\mathbf{B}_s$

$$\mathbf{E} = \mathbf{E}_w + \mathbf{E}_s, \quad \mathbf{B} = \mathbf{B}_w + \mathbf{B}_s \tag{1.6}$$

$$\begin{aligned}
\mathbf{E}_w &= \mathbf{E}_m(\xi)\left[I_0\left(\frac{2\pi\sqrt{1-\beta_w^2}}{\beta_w}\eta\right)\cos\varphi\,\mathbf{i}_z + (1-\beta_w^2)^{-1/2} I_1\left(\frac{2\pi\sqrt{1-\beta_w^2}}{\beta_w}\eta\right)\sin\varphi\,\mathbf{i}_r\right] \\
\mathbf{B}_w &= B_\xi(\xi)\,\mathbf{i}_z - \frac{\eta}{2}\frac{dB_\xi}{d\xi}\mathbf{i}_r + E_m(\xi)\frac{\beta_w}{\sqrt{1-\beta_w^2}} I_1\left(\frac{2\pi\sqrt{1-\beta_w^2}}{\beta_w}\eta\right)\sin\varphi\,\mathbf{i}_\theta
\end{aligned} \tag{1.7}$$

where I_0 and I_1 are Bessel functions of imaginary argument, $\mathbf{i}_z$, $\mathbf{i}_r$, and $\mathbf{i}_\theta$ are unit vectors, and β_w, E_m, and B_ξ depend only on ξ and are given in tables. The expressions which include $E_m(\xi)$ are components of the E_{01} mode in the channel of a cylindrical waveguide with irises. When $\beta_w \approx 1$ Eqs. (1.7) simplify to

$$\mathbf{E}_w = E_m(\xi)\,[\cos\varphi\,\mathbf{i}_z + \pi\eta\beta_w^{-1}\sin\varphi\,\mathbf{i}_r], \quad B_{w,\theta} = E_m(\xi)\pi\eta\sin\varphi \tag{1.8}$$

The space-charge field at the point ξ_i, η_i, where a particle of number i [i = 1, 2, ..., n(t)] is situated, is found by summing the fields produced by all the remaining particles j = 1, 2, ..., n(t), j ≠ i, assuming that the longitudinal component of the current density of the beam is predominant:

$$\begin{aligned}
\mathbf{E}_s(\xi_i, \eta_i) &= A\sum_{j\neq i}[S_0(\eta_i, \eta_j, \varkappa_{ij})\,\mathrm{sign}(\xi_i - \xi_j)\,\mathbf{i}_z + \mu_j S_1(\eta_i, \eta_j, \varkappa_{ij})\,\mathbf{i}_r] \\
B_{s,\theta}(\xi_i, \eta_i) &= A\sum_{j\neq i}\xi_j'\mu_j S_1(\eta_i, \eta_j, \varkappa_{ij})
\end{aligned} \tag{1.9}$$

$$A = Me^2\lambda / (2\pi\varepsilon_0 m_0 c^2 a^2), \quad \mu_j = (1 - (\xi_j')^2)^{-1/2} \tag{1.10}$$

Here a is the radius of the tube, and S_0 and S_1 are the action functions for an infinitely thin ring in an ideally conducting cylindrical tube:

$$S_p(\eta_i, \eta_j, \varkappa_{ij}) = \sum_{k=1}^{\infty} \frac{J_0(\nu_k \lambda a^{-1}\eta_j) J_p(\nu_k \lambda a^{-1}\eta_i)}{J_1^2(\nu_k)} e^{-\nu_k \varkappa_{ij}} \quad (p = 0; 1) \tag{1.11}$$

In Eq. (1.11) j is the index of the ring (of the computer particle), which produces the field, i is the index of a particle, on which the field acts, and $J_0(\nu_k) = 0$, and

$$\varkappa_{ij} = \lambda a^{-1}\mu_j \mid \xi_i - \xi_j \mid \tag{1.12}$$

Most of the computational time is required for calculating the space-charge field (1.9), since the required number of operations is proportional to $n^2(t)$.

2. The simulation is carried out with a constant step Δt, which is a compromise between accuracy and speed of solution. When solving the equations of motion (1.3) we used Adams' extrapolation formula for the velocities of each of the $i = 1, 2, \ldots, n(t)$ particles, which enables one to calculate the right sides uniquely at each step and which has an accuracy at each step of the order of $(\Delta t)^4$. For ξ_i', for example, we have

$$\xi_i'(t + \Delta t) = \xi_i'(t) + \Delta t\, [\, {}^{23}/_{12}\, F_{\xi i}(t) - {}^4/_3\, F_{\xi i}(t - \Delta t) + {}^5/_{12}\, F_{\xi i}(t - 2\Delta t)] \tag{2.1}$$

where the right sides $F_{\xi i}(t - \Delta t)$, $F_{\xi i}(t - 2\Delta t)$ of Eq. (1.3) are calculated in the preceding simulation steps and then kept for the subsequent calculations. We similarly calculate $\eta_i'(t + \Delta t)$, $\alpha_i(t + \Delta t)$.

To calculate the coordinate ξ_i we use an expansion in a power series:

$$\xi_i(t + \Delta t) = \xi_i(t) + \xi_i'(t)\,\Delta t + \xi_i''(t)\,(\Delta t)^2/2 + \xi_i'''(t)\cdot(\Delta t)^3/6 + \xi_i^{(IV)}(t)\,(\Delta t)^4/24 \tag{2.2}$$

with the remaining term of the order of $(\Delta t)^5$. According to the formulas of numerical differentiation

$$\begin{gathered} \xi_i''(t) = F_{\xi i}(t) \\ \xi_i'''(t) = F_{\xi i}'(t) = [F_{\xi i}(t - 2\Delta t) - 4F_{\xi i}(t - \Delta t) + 3F_{\xi i}(t)]\,(2\Delta t)^{-1} \\ \xi_i^{(IV)}(t) = F_{\xi i}''(t) = [F_{\xi i}(t - 2\Delta t) - 2F_{\xi i}(t - \Delta t) + F_{\xi i}(t)](\Delta t)^{-2} \end{gathered} \tag{2.3}$$

Substituting Eqs. (2.3) into Eq. (2.2), we obtain

$$\xi_i(t + \Delta t) = \xi_i(t) + \xi_i'(t)\,\Delta t + {}^1/_4\,(\Delta t)^2\,[\,{}^{19}/_6 F_{\xi i}(t) - {}^5/_3 F_{\xi i}(t - \Delta t) + {}^1/_2 F_{\xi i}(t - 2\Delta t)] \tag{2.4}$$

We calculate $\eta_i(t + \Delta t)$ similarly. The phase φ_i is found from Eq. (1.5); the values of the integral $\Phi(\xi)$ are first tabulated for the whole of the interaction space, so that $\Phi[\xi_i(t)]$ can be calculated at each step by interpolation using the tables. In the drift space $\xi < \xi_0$ we assume $\Phi(\xi) = 0$.

To calculate the coordinates, the velocities, and the phase of a particle at the instant of time $t + \Delta t$ we must know eleven quantities $[\xi(t), \xi'(t), \ldots, F_\alpha(t - 2\Delta t)]$ for each particle. The capacity of the operative memory of a computer of average class enables these quantities to be stored for several hundred particles.

In the first two steps of the simulation ("acceleration"), instead of the Adams' method we used Euler's method for the velocity

$$\xi_i'(t + \Delta t) = \xi_i'(t) + F_{\xi i}(t)\,\Delta t \tag{2.5}$$

[similarly for $\eta_i(t + \Delta t)$ and $\alpha(t + \Delta t)$] and the power series

$$\xi_i(t + \Delta t) = \xi_i(t) + \xi_i'(t)\,\Delta t + F_{\xi i}(t)\,(\Delta t)^2/2 \tag{2.6}$$

for the coordinates [similarly for $\eta_i(t + \Delta t)$].

To calculate the action function (1.11) we constructed a grid region with respect to the three variables $(\eta_i, \eta_j, \varkappa_{ij})$. Before starting the simulation we drew up tables of values of S_p ($p = 0, 1$) at the nodes of the

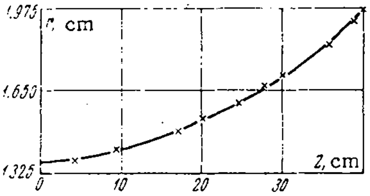

Fig. 1

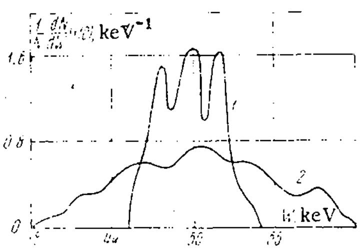

Fig. 2

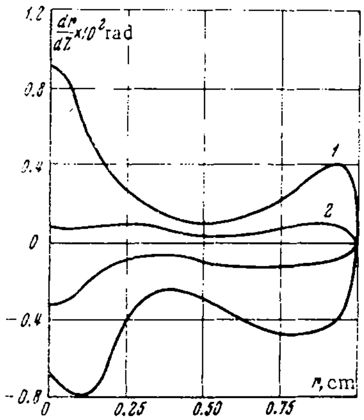

Fig. 3

grid. With respect to $\varkappa$ (1.12) the step of the grid $\Delta\varkappa$ was chosen to be constant and to be such that the whole of the bunch was covered by the grid:

$$\varkappa_{ij} = x_{ij}\,\Delta\varkappa \qquad (0 \leqslant x_{ij} \leqslant N_\varkappa) \tag{2.7}$$

where $N_\varkappa$ is the number of nodes of the grid with respect to variable $\varkappa$. As far as the radius is concerned it is best to choose a grid the step of which increases with distance from the axis. This enables one to have more nodes and to calculate the field more accurately in the region filled by the beam, since the beam is usually concentrated in the region of the axis of the system. Hence, the radius nodes are chosen with a unit step with respect to the variable y, which is related to η by the expression

$$\eta = (b/\lambda)\,(e^{k_y y} - 1)\,(e^{k_y N_\eta} - 1)^{-1} \qquad (0 \leqslant y \leqslant N_\eta) \tag{2.8}$$

where N_η is the number of nodes of the grid with respect to y. The axis of the tube corresponds to y = 0, and the internal radius of the iris b corresponds to $y = N_\eta$. The distance between neighboring nodes with respect to the variable η according to Eq. (2.8) increases as $\exp(k_y y)$. By varying parameter k_y, one can change the degree of nonuniformity of the grid.

Tables of the action functions were constructed in practice with respect to the variables y_i, y_j, and x_{ij} at the nodes $y_i, y_j = 0, 1, 2, \ldots, N_\eta$; $x_{ij} = 0, 1, 2, \ldots, N_\varkappa$. Since the function S_0 is symmetrical with respect to η_i, η_j, the table of $S_0(y_i, y_j, x_{ij})$ is only drawn up for values of $y_i \geq y_j$. For $x_{ij} = 0$ we assume $S_0(y_i, y_j, 0) = 0$, $S_1(y_i, y_j, 0) = S_1(y_i, y_j, 1)$. The total number of nodes in the tables of S_0 and S_1 is of the order of $1.5\,(N_\eta + 1)^2\,(N_\varkappa + 1)$.

During the simulation procedure with respect to the coordinates η_i, η_j we calculated y_i and y_j from Eq. (2.8), and we calculated x_{ij} from Eq. (2.7). The values of the action function S_p, which occur in Eq. (1.9), at the points y_i, y_j, and x_{ij} were found using linear interpolation between the table components:

$$\begin{gathered} S_p(\eta_i, \eta_j, \varkappa_{ij}) = S_p(y_i, y_j, x_{ij}) = S_p(y_i^{(0)}, y_j^{(0)}, x_{ij}^{(0)}) + \Delta S_p \\ \Delta S_p = \frac{\partial S_p}{\partial y_i}(y_i - y_i^{(0)}) + \frac{\partial S_p}{\partial y_j}(y_j - y_j^{(0)}) + \frac{\partial S_p}{\partial x_{ij}}(x_{ij} - x_{ij}^{(0)}) \\ p = (0;\,1) \end{gathered} \tag{2.9}$$

where the superscript (0) denotes the integral part of the number, and the derivatives represent the difference between the action functions at the nodes which are adjacent with respect to the corresponding variables, since the distance between neighboring nodes $\Delta y_i^{(0)} = \Delta y_j^{(0)} = \Delta x_{ij}^{(0)} = 1$. For values $x_{ij}^{(0)} > N_\varkappa$ the functions $S_p(\eta_i, \eta_j, \varkappa_{ij})$ are assumed to be zero.

The major part of the calculations using Eqs. (1.9) and (2.9) can be carried out in advance, so that the required number of operations is reduced considerably. This enables one to simulate important practical modes of operation on a computer of average class in an acceptable time.

3. The time taken to compute a single step on an M-220 computer increases from 27 sec for n = 100 to 432 sec for n = 400. Figures 1-3 show the results obtained. We injected a single-energy bunch with an initial particle kinetic energy W_0 and a constant space-charge density ρ. For Fig. 1 the initial radius of the beam was 1.37 cm, and for Figs. 2 and 3 the initial radius was 1 cm. For a uniformly charged beam

$$\rho = Men\,/\,(\pi\eta_m^2\xi_m\lambda^3) \tag{3.1}$$

where ξ_m, η_m are the dimensionless length and the dimensionless maximum radius of a bunch. It was assumed that over the whole interaction space $B_{w,\xi}(\xi) = \text{const}$.

Figure 1 shows the increase in the radius $r = \lambda\eta_m$ of a proton beam due to the action of space-charge forces when drifting in free space in the direction of axis. For this case W_0 = 700 keV, $\rho = 0.56 \cdot 10^{-4}$ C/m^3, and n = 50, and the parameters of the grid were $k_y = 0.25$, $N_\eta = 13$, and $N_\varkappa = 25$. In Fig. 1 the continuous curve was calculated from the analytical relation given in [7], and the crosses represent the results of the numerical experiment. The disagreement does not exceed 1%. Figure 2 shows the distribution density dN/dW of the number of particles N(W) with respect to the energy W after passing through a drift of length 4.5 cm; the initial energy W_0 = 50 keV, the focussing magnetic field $B_\xi = 3.522$, and $\rho = 4.1 \cdot 10^{-4}$ C/m^3 for curve 1 and $1.4 \cdot 10^{-3}$ C/m^3 for curve 2. Because of the acceleration of the "leading" particles and the slowing of the "trailing" particles of a bunch the initially single-energy bunch exhibits a spread in energy. As the charge density increases, the energy spectrum broadens. A comparison of curves 1 and 2 (Fig. 2) shows that an increase in the space-charge density by a factor of 3 causes an increase in the absolute energy spread from 9 to 24 keV.

The repulsive Coulomb forces have a considerable effect on the transverse motion of the particles. A suitable characteristic of the radial divergence of the beam is the quantity

$$\sigma = \iint d\eta \, d\eta_\xi, \qquad \eta_\xi \equiv d\eta / d\xi$$

In Fig. 3 curves 1 and 2 limit the region occupied by the representative points of the particles of the bunch* passing through the drift space of length 5 cm, $\rho = 1.4 \cdot 10^{-3}$ C/m^3, $B_\xi = 3.522$, and W_0 = 50 keV for curve 1 and 200 keV for curve 2. It can be seen that an increase in the initial energy of the particles W_0 by a factor of 4 leads to a reduction in the area of the region occupied by the representative points of the particles of the bunch, i.e., of the quantity σ, by a factor of approximately 3.5. This is due to a reduction in the repulsive Coulomb forces as the energy of the particles increases.

Consider the effect of space charge on the bunching of the particles in microwave electromagnetic fields. The external high-frequency field was given by the parameters $E_m(\xi)$ = const = 2.97, $\beta_w(\xi)$ = const = 1. We injected a bunch with initial phase length $\Delta\varphi = 0.12\pi$ rad and energy W_0 = 125 keV. While the energy of the bunch was increasing to 1 MeV, the longitudinal Coulomb repulsion increased the phase length of the bunch to 0.18π for an initial space-charge density $\rho = 4.5 \cdot 10^{-3}$ C/m^3 and to 0.22π for $\rho = 7.5 \cdot 10^{-3}$ C/m^3.

LITERATURE CITED

1. S. P. Lomnev, Calculation and Investigation of Electrophysical Apparatus and Phenomena on Digital Computers [in Russian], Computational Center, Academy of Sciences of the USSR (1965).
2. V. A. Enal'skii and V. V. Osipov, Computer simulation of an accelerator process in a high-current ion linear accelerator, Zh. Prikl. Mekh. Tekh. Fiz., No. 5 (1967).
3. G. W. Petersen and W. J. Gallagher, An analysis of travelling-wave prebunchers, IEEE Trans. Nucl. Sci., 16, No. 3, Pt. 1 (1969).
4. C. B. Williams and M. H. MacGregor, Space charge effects in high current linear electron accelerator injection systems, IEEE Trans. Nucl. Sci., 14, No. 3 (1967).
5. A. Benton, R. Chasman, and C. Agritellis, Computer calculations of the effect of space charge on longitudinal beam dynamics in proton linear accelerators, IEEE Trans. Nucl. Sci., 14, No. 3 (1967).
6. I. S. Berezin and N. P. Zhidkov, Computational Methods [in Russian], Nauka, Moscow, (1966).
7. S. I. Molokovskii and A. D. Sushkov, Intense Electron and Ion Beams [in Russian], Énergiya, Leningrad (1972).
8. I. M. Kapchinskii, Particle Dynamics in Resonance Linear Accelerators [in Russian], Atomizdat, Moscow (1966).

*The term "representative points of the particles of the bunch" was introduced in [8] and denotes the representation of the particles of a bunch in phase space coordinates {r, dr/dz}.